IJPSR (2020), Volume 11, Issue 11 (Research Article)

INTERNATIONAL JOURNAL OF PHARMACEUTICAL SCIENCES AND RESEARCH

Received on 12 February 2020; received in revised form, 29 March 2020; accepted, 31 March 2020; published 01 November 2020

HELICOBACTER PYLORI INFECTION: A BIOINFORMATIC APPROACH

Ashwini Prasad [1], Govindaraju Shruthi [1], P. Sushma [1], Anisha S. Jain [1], D. Chandan [1], M. N. Nagendra Prasad [2], Shiva Prasad Kollur [3], Chandrashekar Srinivasa [4] and Chandan Shivamallu [*1]

Department of Water & Health [1], Faculty of Life Sciences, JSS Academy of Higher Education & Research, Sri Shivarathreeshwara Nagara, Mysore - 570015, Karnataka, India.
Department of Biotechnology [2], JSS Science and Technology University, Sri Jayachamarajendra College of Engineering, Mysore - 570015, Karnataka, India.
School of Arts and Sciences, Amrita Vishwa Vidyapeetham, Mysuru Campus - 570026, Karnataka, India.
Department of Biotechnology [4], Davangere University, Davanagere - 577007, Karnataka, India.

Keywords:

In-silico Analysis, Molecular Docking, Molecular Interaction, *Helicobacter pylori*

Correspondence to Author:
Dr. Chandan Shivamallu

Assistant Professor and Course Coordinator, Division of Biotechnology and Bioinformatics, Department of Water & Health, Faculty of Life Sciences, JSS Academy of Higher Education & Research, Sri Shivarathreeshwara Nagara, Mysore - 570015, Karnataka, India.

E-mail: chandans@jssuni.edu.in

ABSTRACT: *Helicobacter pylori* causative agent of acid peptic disease is a microaerophilic, spiral-shaped, gram-negative bacteria found in the gastric epithelium that may also lead to complications such as chronic gastritis, mucosa-associated lymphoid tissue (MALT) lymphoma, gastroduodenal ulcer and adenocarcinoma in stomach. Plantbioactives have always been potential therapeutics. Usage of modern bioinformatic tools plays a vital role in exploiting the potentials of alternative therapeutic molecules in managing diseases like peptic ulcers and their complications. The *in-silico* evaluation was carried out using molecular docking of the quorum sensing proteins of *H. pylori* with the ligand β-sitosterol obtained from the silver nanoparticles of *Acorus calamus* L. Among several given quorum sensing proteins the molecular interaction with the ligand β-sitosterol showed a high binding affinity with *DnaA*, *PhnB*, *ToxB* and *Sip* proteins. The results obtained from molecular interaction study revealed that the ligand β-sitosterol will be readily taken up by the organism, thereby facilitating easy inhibition or inactivation of quorum sensing molecules *ToxB*, *DnaA*, *PhnB*, and *Sip*, making it a novel therapeutic alternative to treat *H. pylori* infections.

INTRODUCTION: The acid peptic disease is a condition due to frequent pathogenic actions involving excessive secretion of acid resulting in acid reflux, thereby damaging esophageal mucosa and laryngeal tissue. Further peptic ulcer condition is complicated by secretion of pepsin and gastric acid that damages mucosa and causes ulcers in the lower esophagus and duodenum region.

QUICK RESPONSE CODE

DOI: 10.13040/IJPSR.0975-8232.11(11).5469-83

This article can be accessed online on www.ijpsr.com

DOI link: http://dx.doi.org/10.13040/IJPSR.0975-8232.11(11).5469-83

This acidity related disease hampers the lifestyle quality of individuals leading to rampant morbidity and mortality. Even in a developed country like the US, 40% of youth frequently complain of Heartburn, highlighting gastroesophageal reflux disorder (GERD) as one of the most common disorders [1].

Presently, there are 3 lines of antibiotic therapies for the treatment of *H. pylori*-related complications *viz*., Concomitant & hybrid therapy, Bismuth quadruple & Levofloxin therapy, and Culture guided therapy [2]. The antibiotics of choice for treating *H. pylori* infections are metronidazole, tetracycline, clarithromycin, amoxicillin, fluoro-quinolones, tinidazole along with bismuth salts or

proton pump inhibitors (PPIs). Resistance to particular antibiotics has made to use the combination of drugs in areas where there is more prevalence of resistance to a single antibiotic [3].

H. pylori is an S-shaped, gram-negative bacteria with sheathed and polar flagella, which grow in microaerophilic conditions and is varied by its turns/spirals and size [4]. *H. pylori* are most likely to spread from person to person through oral-oral, gastro-oral, or fecal-oral route. Other sources of transmission recorded in the literature also include contaminated water, iatrogenic modes, especially during endoscopy and rarely zoonotic transmission, too, though direct contact with the individuals remains the most prevalent spreading method [5]. One of the most common bacteria that infect the world's 50% of the population leading to peptic ulcer and adenocarcinoma is *H. pylori* [6]. Acquisition of *H. pylori* infection is controlled by the persistence of infection and also infection rate loss [7].

Plant mediated synthesis of nanobactericides is a protocol which exploits plant or their products to synthesize the desired class of nanobactericides [8]. In a plant-mediated synthesis of nanobactericides, there are two different types of extracellular synthesis, which involves the extraction of plant products in the form of aqueous extract and using it to synthesize nanobactericides [9]. Hence the present study makes a primary attempt to prosper the fact to develop novel nanobactericides against the treatment of *H. pylori* biofilm formation. The developed nanobactericides are synthesized using a facile route by exploring the herbal plants, which are reported to have a high therapeutic index. One of the advantages of developing plant-based nanobactericides is that it may protect the host immune system and can minimize the risks of drug resistance to prevent latent infections. As the pathogens can inhabit various host niches and the conventional medicines often fail or damage the host self-defense, which may lead to a compromised immune system. Hence, the use of nanobactericides can be highly advantageous.

Quorum sensing in *H. pylori* is an evident phenomenon. Still, it lacks in understanding the detailed mechanism of various proteins involved in quorum sensing and requires in-depth and vast research in the field. Currently, only a few quorum sensing genes have been annotated, which includes *LuxS* and *ToxB.* These are the only two quorum sensing proteins which have been structurally annotated and the sequence of which is currently available in Protein Data Bank and GenBank.

The other known quorum sensing proteins **Table 1** requires structural annotation and elucidation of the mechanism of action, which has been carried out in the current study through *in-silico* annotation and analysis using structural elucidation and molecular interaction studies and is the main focus of the current research work.

TABLE 1: QUORUM SENSING PROTEINS OF *H. PYLORI*

S. no.	Gene	Protein
1	*LuxS*	S-ribosylhomocysteinelyase
2	*PhnA*	Anthranilate synthase component I
3	*PhnB*	Anthranilate synthase component II
4	*PhnC*	3-deoxy 7-phosphoheptulonate synthase
5	*ToxB*	GTP cyclohydrolase-II
6	*ToxE*	Diaminohydroxyphosphoribosyl amino pyramidinedeaminase
7	*SpSB*	Signal Peptidase I
8	*Eep*	Zinc metalllo protease/ regualator of sigma E protease
9	*CcfA*	Membrane Protein insertaseYidc/ Oxal family membrane protein insertase
10	*Sec*	Fused signal recognition particle receptor
11	*Sip*	Signal Peptidase I
12	*FlicC*	Flagellin B
13	*FlicA*	RNA Polymerase sigma factor for flagellar operon FliA
14	*MotA*	Flagellar motor protein
15	*DnaA*	Chemosomal replication initiator protein

*Note: Proteins obtained from cross-reference of KEGG and GenBank.

LuxS is a well-known quorum sensing molecule involved in the production of autoinducer II, which is found to be involved in the formation of lesions, which results in the easy access of the pathogen

into the host cell. Thereby further spreading the infection to the nearby cells and tissues, leading to host tissue necrosis. The inhibition of *LuxS* prevents the ability of the organism to invade host tissue/cells through cytolysis [10].

ToxB, GTP cyclohydrolase is an essential protein involved in the acclimatization of *H. pylori* in acidic conditions. This protein prevents the degradation of the bacterial cell wall in the host intestine and helps in the growth and homeostasis of the bacteria. The particular protein lays the foundation for the establishment of biofilm in the host, thereby directly influencing the propagation of infection and invasion into the host cell [11].

Quorum sensing pathway of *H. pylori* has been annotated using *in-silico* tools such as KEGG (Kyoto Encyclopedia for Genes and Genomics) wherein, *LuxS, DnaA, PhnA, PhnB, FlaB, ToxB* and *Sip* were found to be the key quorum sensing molecule involved in biofilm formation in *H. pylori* **Fig. 1**.

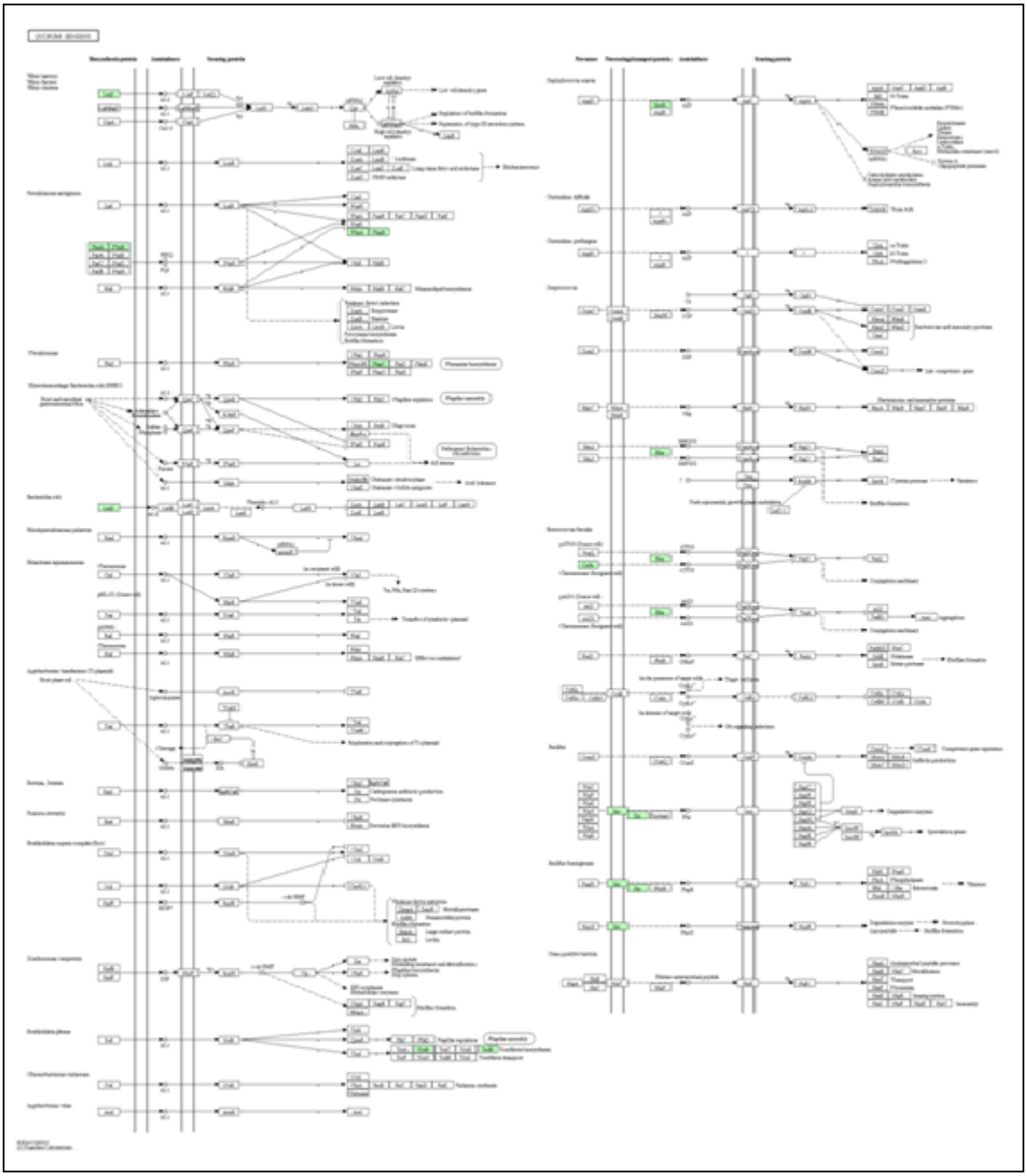

FIG. 1: EXHIBITING THE QUOROM SENSING OF *H. PYLORI* INVOLVING QUORUM SENSING MOLECULES *LUXS, PHNA, PHNB, FLAB, TOXB* AND *SIP* OF *H. PYLORI* (IN GREEN COLOR). (IMAGE COURTESY- KEGG PATHWAY DATABASE: HPY02024)

MATERIALS AND METHODS:

Structural Annotation of Protein of *H. pylori:* Structure of *LuxS* and *ToxB* proteins were procured from Protein Data Bank (PDB) and were found to be fit for further *in-silico* analysis without the requirement of any further modifications. The structures of *DnaA, PhnA, PhnB, FliC*, and *Sip* were unannotated and required ab-initio structure building. The sequences of these five proteins were obtained from the GenBank database of *H. pylori* proteome and were subject to structure prediction using the Raptor-X tool [11].

Binding Site Prediction of Proteins: The binding sites of *LuxS* and *ToxB* proteins were analyzed and obtained through the ligand explorer tool. The amino acid residues of the binding sites of structurally annotated proteins *DnaA, PhnA, PhnB, FliC*, and *Sip* were predicted using B Spread tool of Yang Zhang Lab [12, 14].

Ligand Preparation: The 3-dimensional structure of the ligand β-sitosterol was prepared in two steps, in the first step; the 2-dimensional structure of β-sitosterol was drawn in Chemdraw (v.8.0) software and was saved as .cdx file. In the second step, 2 dimensional structure of β-sitosterol was converted to a 3-dimensional structure by the addition of 3D coordinates to the structure and was made explicit, using Openbabel software [15].

Molecular Docking: The molecular interaction studies of the prepared ligand with all the seven proteins were performed using rigid docking studies using Autodock suite (v.4.2.6) using genetic algorithm setting to check the interaction of β-sitosterol with the proteins where the grid was set for the binding site, and the protein macromolecule was set as a rigid molecule, and the various possible confirmations of ligand were generated[16].

Visualization: Upon completion of molecular docking, the various confirmations of a ligand in association to respective proteins were visualized to analyze various interactions of ligands with the binding site residues of the protein using UCSF Chimera visualization tool, based on the type of interaction, a number of interactions and docking score, the best-fit orientation of the ligand was selected [16].

RESULTS AND DISCUSSION:

***In-silico* Analysis:**

Structural Annotation of Proteins of *H. pylori:* The structure of *LuxS* and *ToxB* obtained from Protein Data Bank did not require further refinement other than removal of the bound ligand, structures of *LuxS* and *ToxB* devoid of a ligand is represented in **Fig. 2** and **Fig. 4** respectively. The structures of *DnaA, PhnA, PhnB, FliC*, and *Sip* obtained from RaptorX were validated through a Ramachandran plot. The validated structures which obeyed structure-activity relationship were selected and the structures of *DnaA, PhnA, PhnB, FliC*, and *Sip* are represented in **Fig. 9 - Fig. 13** respectively.

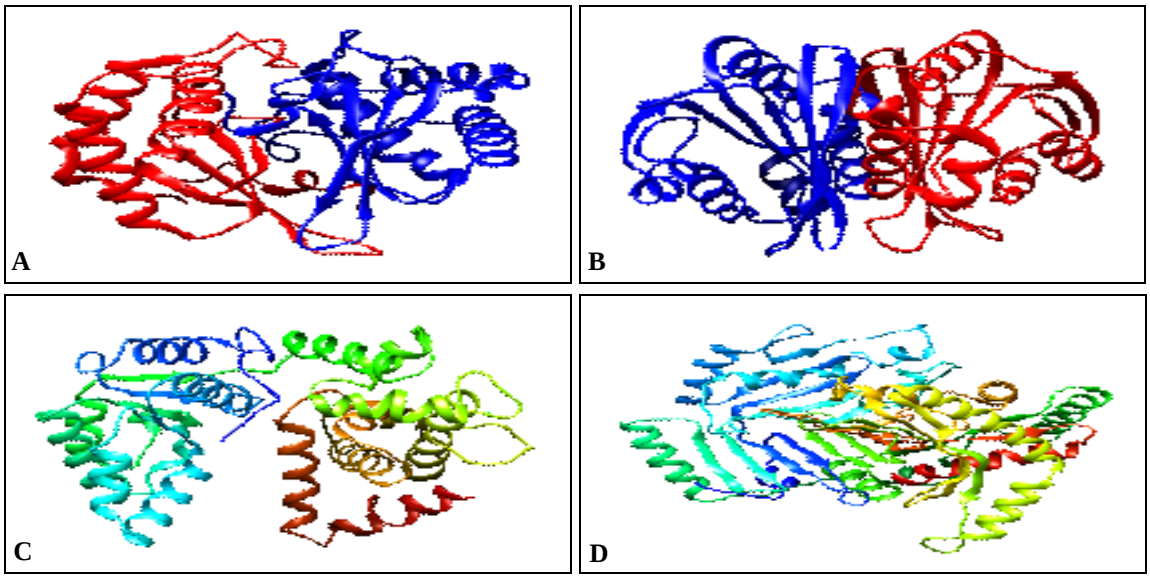

FIG. 2: A: STRUCTURE OF *LUXS (PDB ID:1J6X)* DEVOID OF COFACTOR ZN, REPRESENTED IN RIBBON PRESET; B: STRUCTURE OF *TOXB (PDB ID:4RL4)* DEVOID OF LIGAND PPV, REPRESENTED IN RIBBON PRESET; C: STRUCTURE OF *DNAA* REPRESENTED IN RIBBON PRESET; D: STRUCTURE OF *PHNA* REPRESENTED IN RIBBON PRESET

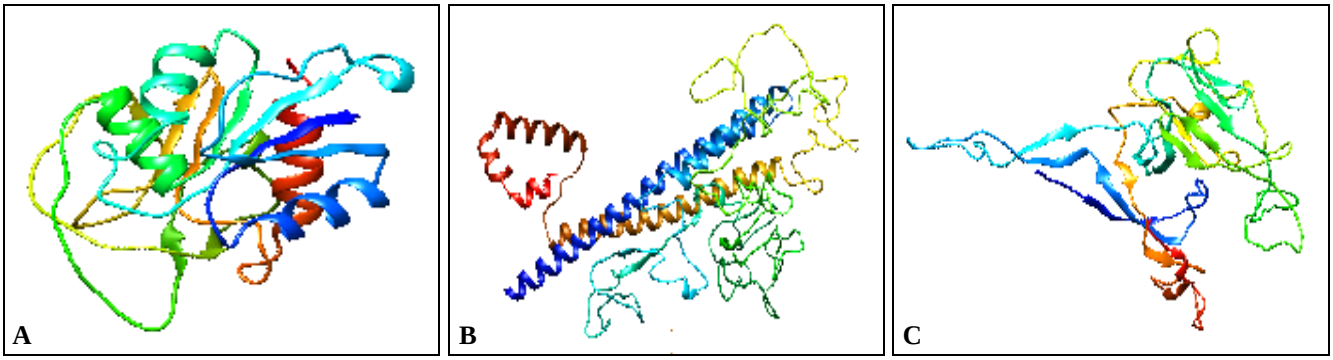

FIG. 3: A: STRUCTURE OF *PHNB* REPRESENTED IN RIBBON PRESET; B: STRUCTURE OF *FLIC* REPRESENTED IN RIBBON PRESET; C: STRUCTURE OF *SIP* REPRESENTED IN RIBBON PRESET

Validation of Protein Structures: The structures of *DnaA, PhnA, PhnB, FliC,* and *Sip* procured from RaptorX were validated through Ramachandran plot analysis using Phenix (v.1.13) and are depicted in **Fig. 4 - Fig. 8**. Only structures which had at least 95 percent of the residues in the favorable region and around 2 percent of the residues in the allowed regions were considered to be fit for molecular interaction studies.

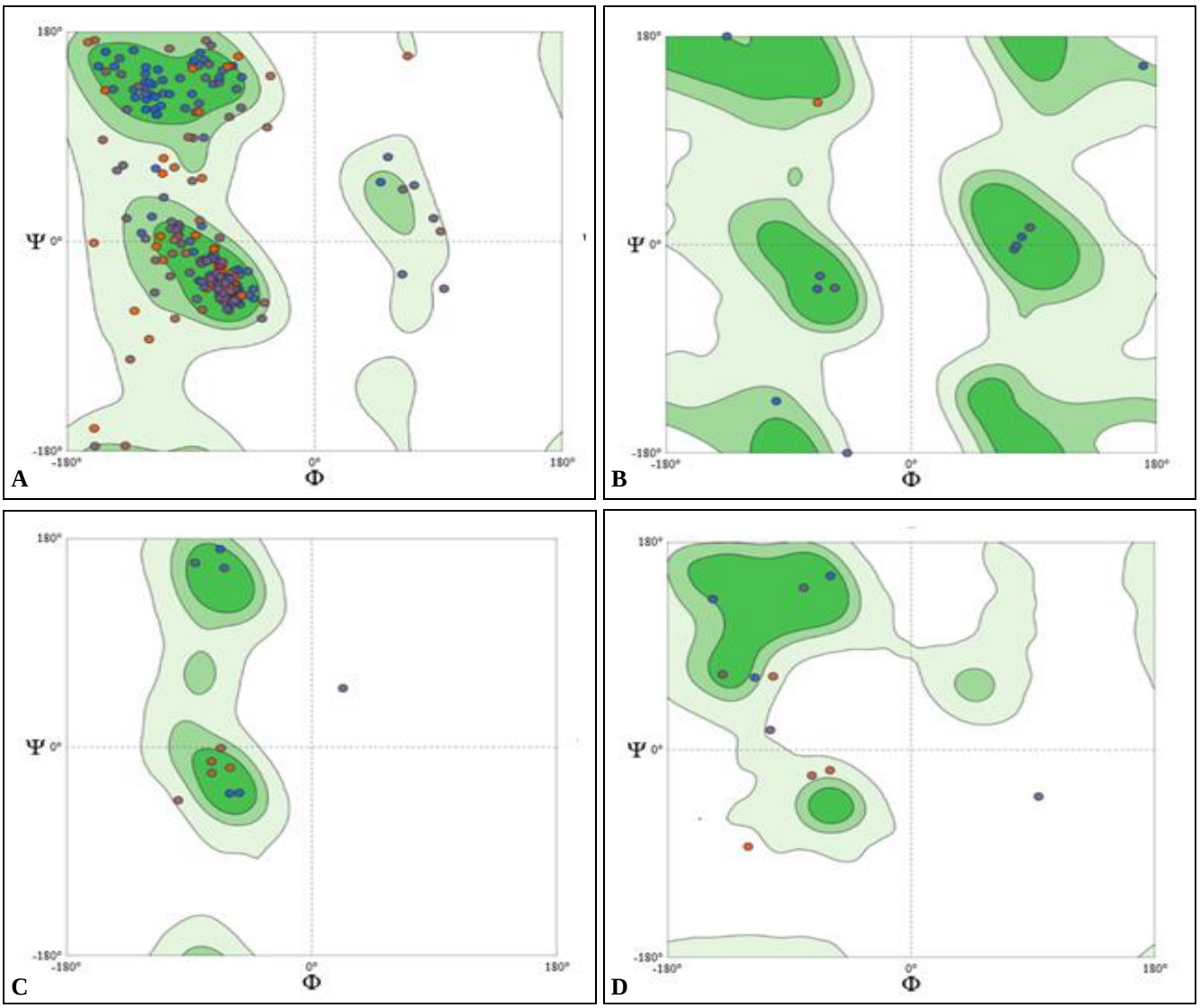

FIG. 4: RAMACHANDRAN PLOT PREDICTION FOR STRUCTURE OF *DNAA*; A: GENERAL PLOT; B: GLYCINE RESIDUES OF *DNAA* STRUCTURE; C: PROLINE RESIDUES OF *DNAA* STRUCTURE; D: PRE-PROLINE RESIDUES OF *DNAA* STRUCTURE

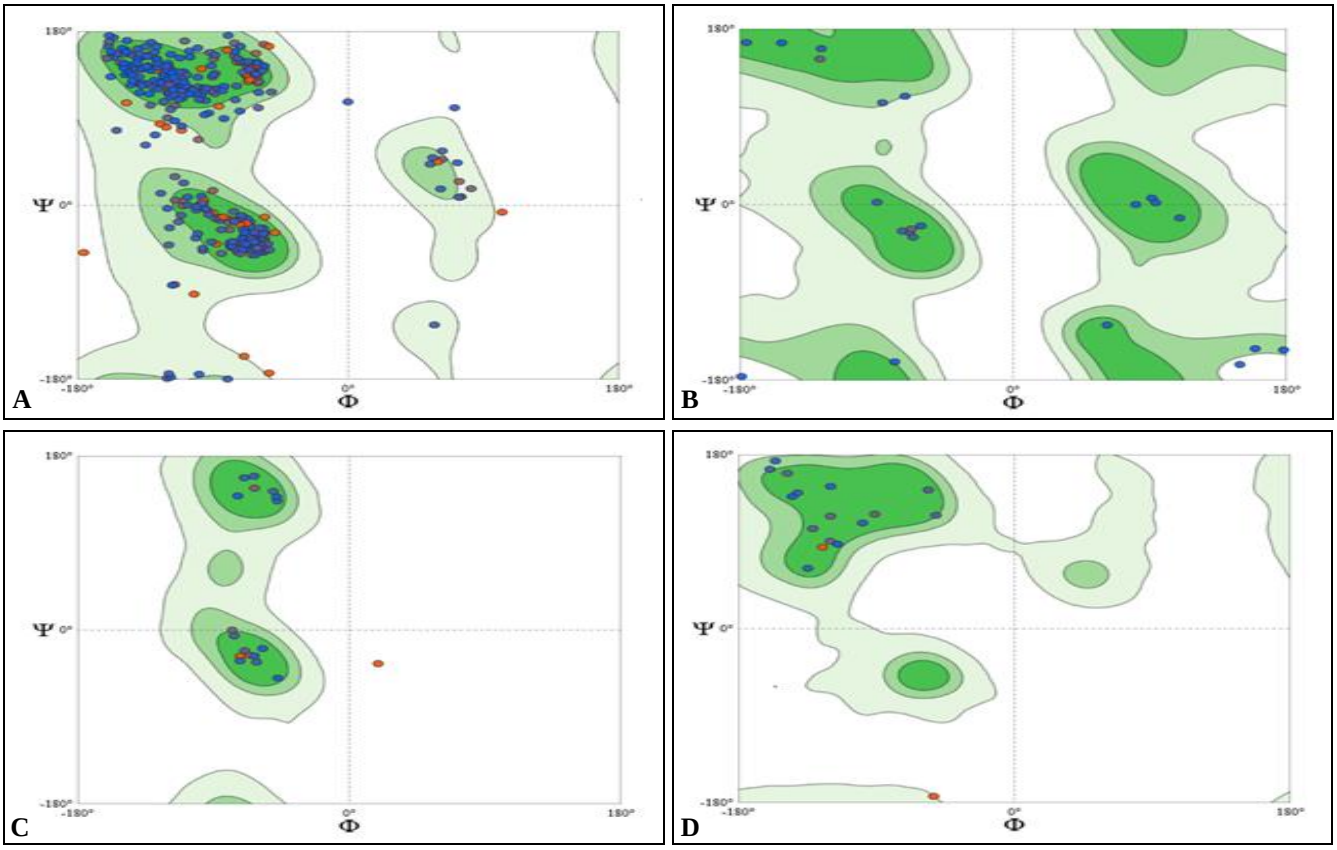

FIG. 5: RAMACHANDRAN PLOT PREDICTION FOR STRUCTURE OF *PHNA*; A: GENERAL PLOT; B: GLYCINE RESIDUES OF *PHNA* STRUCTURE; C: PROLINE RESIDUES OF *PHNA* STRUCTURE; D: PRE-PROLINE RESIDUES OF *PHNA* STRUCTURE

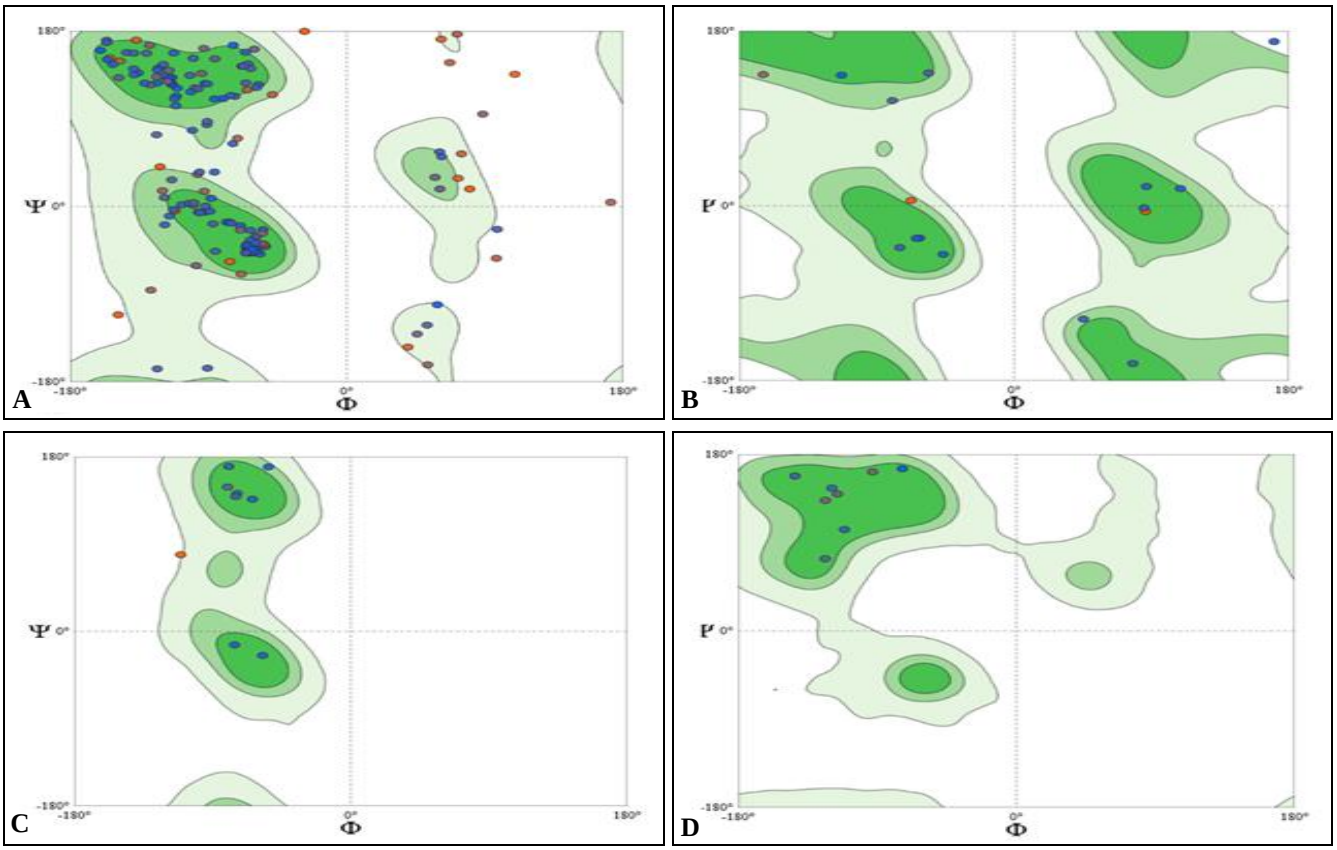

FIG. 6: RAMACHANDRAN PLOT PREDICTION FOR STRUCTURE OF *PHNB*; A: GENERAL PLOT; B: GLYCINE RESIDUES OF *PHNB* STRUCTURE; C: PROLINE RESIDUES OF *PHNB* STRUCTURE; D: PRE-PROLINE RESIDUES OF *PHNB* STRUCTURE

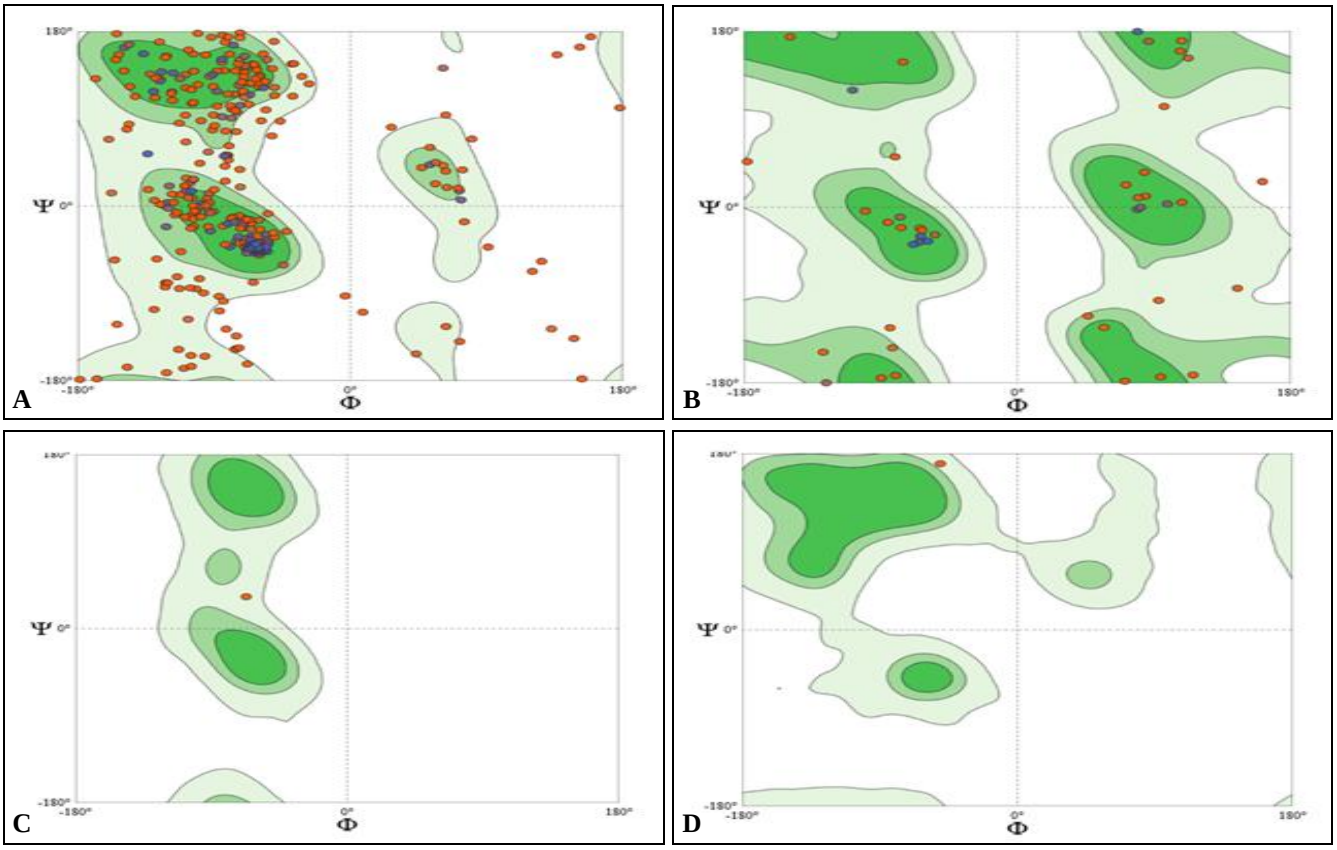

FIG. 7: RAMACHANDRAN PLOT PREDICTION FOR STRUCTURE OF *FLIC*; A: GENERAL PLOT; B: GLYCINE RESIDUES OF *FLIC* STRUCTURE; C: PROLINE RESIDUES OF *FLIC* STRUCTURE; D: PRE-PROLINE RESIDUES OF *FLIC* STRUCTURE

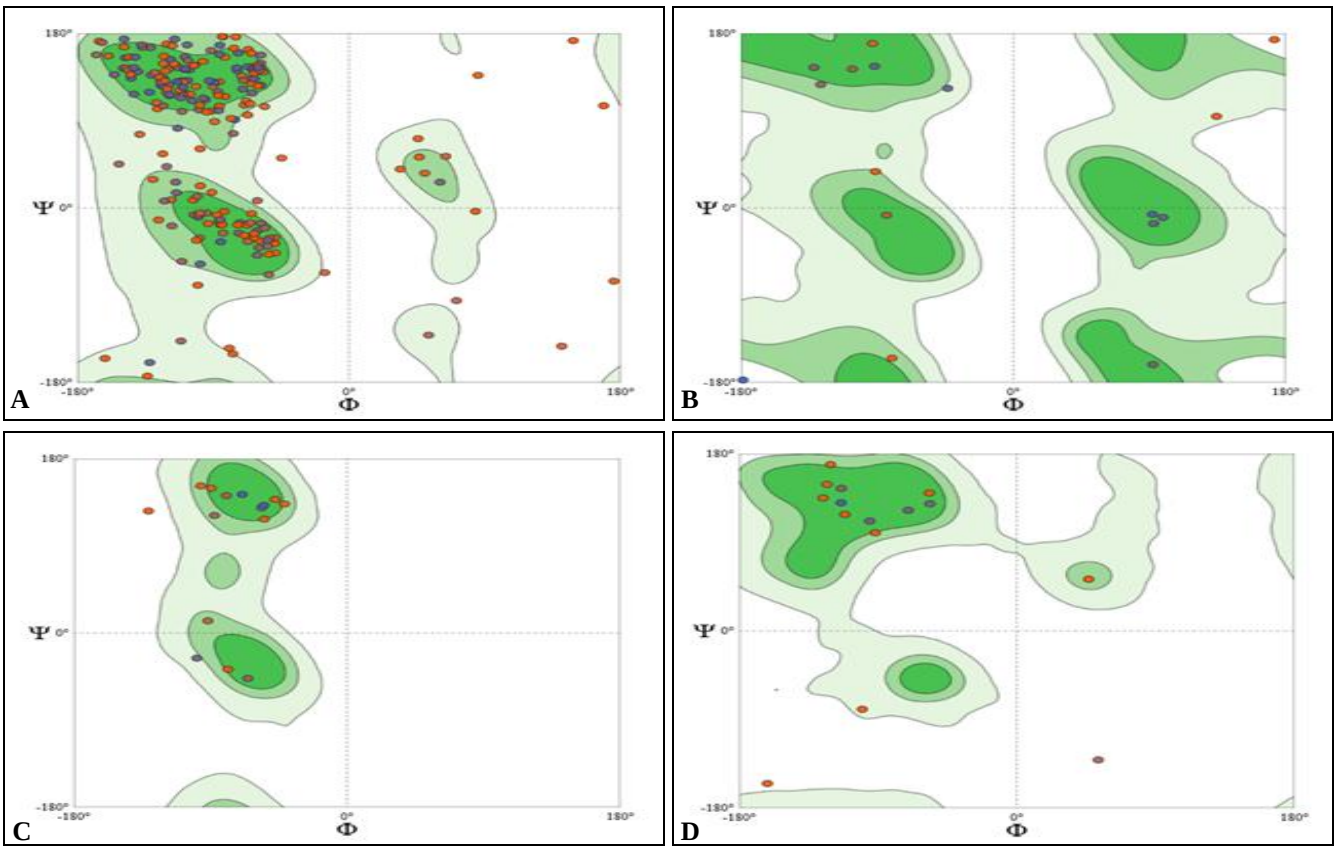

FIG. 8: RAMACHANDRAN PLOT PREDICTION FOR STRUCTURE OF *SIP*; A: GENERAL PLOT; B: GLYCINE RESIDUES OF *SIP* STRUCTURE; C: PROLINE RESIDUES OF *SIP* STRUCTURE; D: PRE-PROLINE RESIDUES OF *SIP* STRUCTURE

Binding Site Prediction of Structurally Annotated Proteins: A congruence binding site obtained from various algorithms of Bspread was considered for molecular interaction studies of *DnaA, PhnA, PhnB, FliC,* and *Sip*. Each protein showed involvement of at least six residues information of the binding site. The binding sites of respective proteins have been depicted in **Fig. 9 - Fig. 13**.

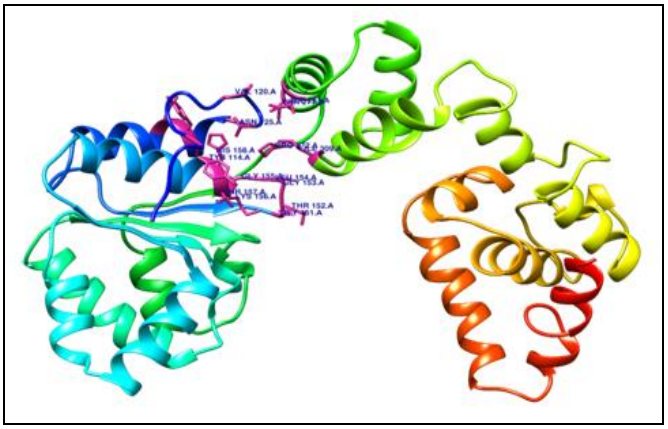

FIG. 9: EXHIBITING BINDING SITE RESIDUES OF *DNAA*, DEPICTED IN PINK COLOR WITH RESPECTIVE RESIDUE LABELS IN BLUE

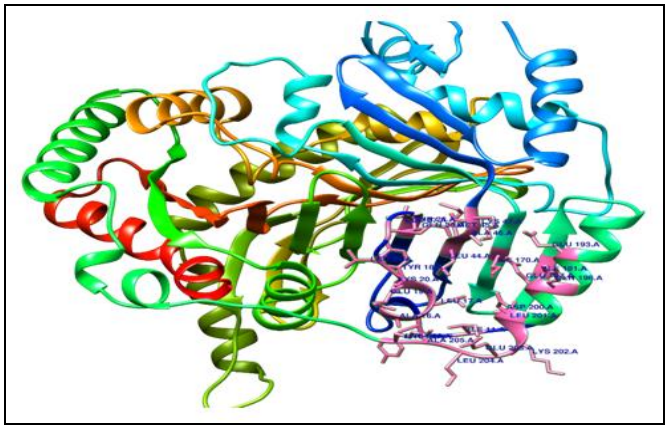

FIG. 10: EXHIBITING BINDING SITE RESIDUES OF PHNA, DEPICTED IN PINK COLOR WITH RESPECTIVE RESIDUE LABELS IN BLUE

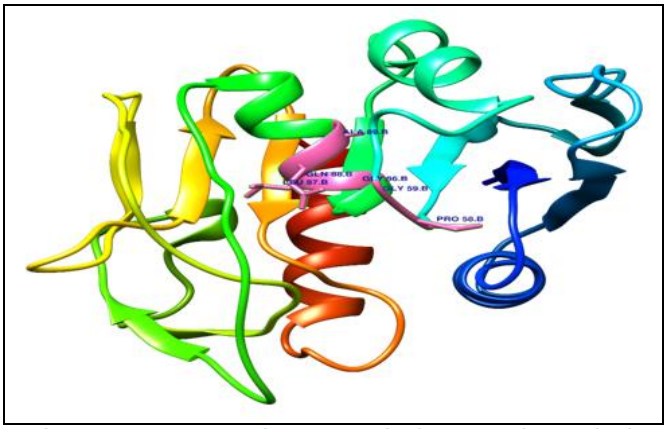

FIG. 11: EXHIBITING BINDING SITE RESIDUES OF PHNB, DEPICTED IN PINK COLOR WITH RESPECTIVE RESIDUE LABELS IN BLUE

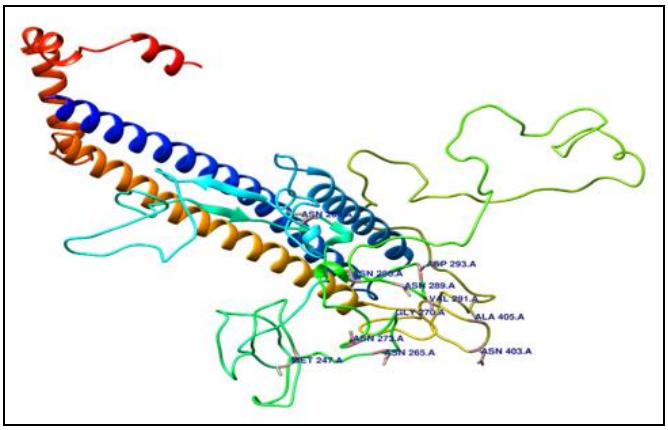

FIG. 12: EXHIBITING BINDING SITE RESIDUES OF FLIC, DEPICTED IN PINK COLOR WITH RESPECTIVE RESIDUE LABELS IN BLUE

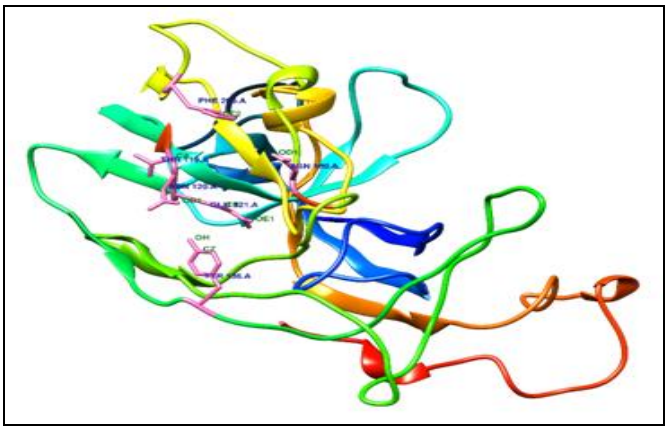

FIG. 13: EXHIBITING BINDING SITE RESIDUES OF SIP, DEPICTED IN PINK COLOR WITH RESPECTIVE RESIDUE LABELS IN BLUE

Molecular Interaction Studies: The molecular interaction studies performed through molecular docking of β-sitosterol against the quorum sensing proteins *LuxS, ToxB, DnaA, PhnA, PhnB, FliC,* and

Sip, exhibited exceptionally high binding affinity and molecular interaction with proteins *ToxB*, *DnaA*, *PhnB*, and *Sip*, whereas, β-sitosterol did not show significant binding and interactions with *LuxS*, *PhnA*, and *FliC*. The annotation of molecular interaction of β-sitosterol with *ToxB*, *DnaA*, *PhnB*, and *Sip* visualized using UCSF Chimera is depicted in **Fig. 14 -Fig. 23**.

Interaction of β-sitosterol with *ToxB:* β-sitosterol was found to bind *ToxB* at a binding site specified above along with additional amino acid residues surrounding the binding site of *ToxB*, overall of β-sitosterol was found to interact with Val49, Arg50, Leu51, His52, Ile87, Leu137, Met145, Thr149, Asn150, Asn151, Met154, and Leu 169.

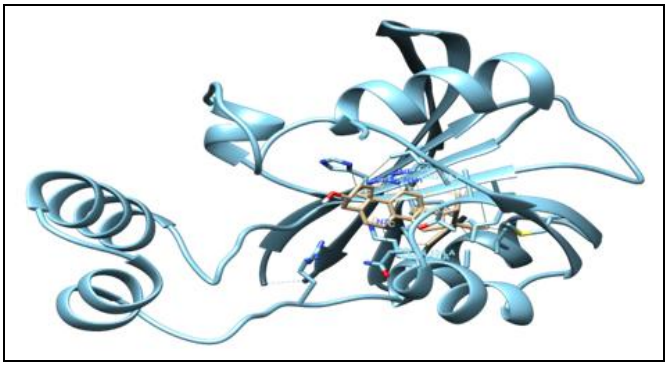

FIG. 14: MOLECULAR INTERACTION OF β-I WITH *TOXB* BINDING SITE DEPICTED IN RIBBON PRESET WITH β-SITOSTEROL DEPICTED IN GOLDEN HUE

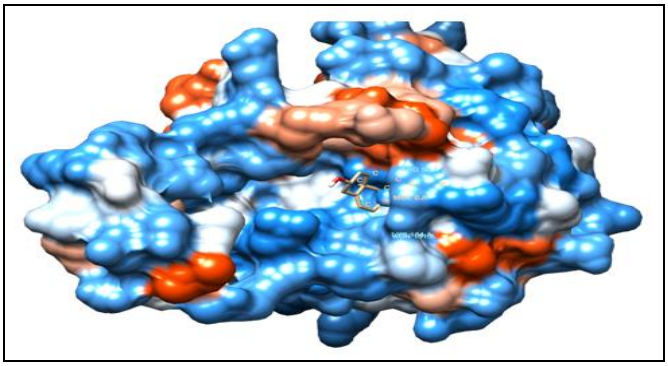

FIG. 15: DEPICTION OF β-SITOSTEROL INTEGRATED IN *TOXB* BINDING POCKET VISUALIZED UPON REPRESENTATION OF *TOXB* IN HYDROPHOBICITY SURFACE MODEL

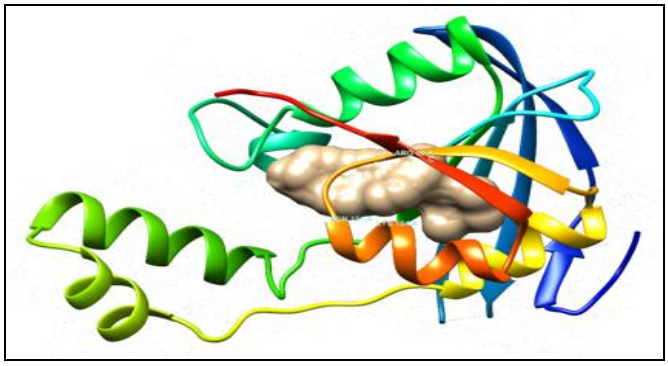

FIG. 16: DEPICTION OF β-SITOSTEROL INTEGRATED IN *TOXB* BINDING POCKET VISUALIZED UPON REPRESENTATION OF β-SITOSTEROL IN HYDRO-PHOBICITY SOLID SURFACE MODEL AND *TOXB* IN DOTTED HYDROPHOBICITY SURFACE

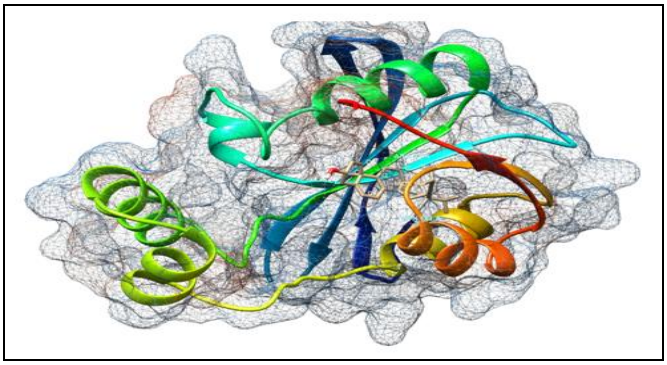

FIG. 17: DEPICTION OF β-SITOSTEROL INTEGRATED IN *TOXB* BINDING POCKET VISUALIZED UPON REPRESENTATION OF *TOXB* IN HYDROPHOBICITY SURFACE MESH MODEL, WHERE β-SITOSTEROL IS DEPICTED IN CYLINDER MODEL WITH GOLDEN HUE

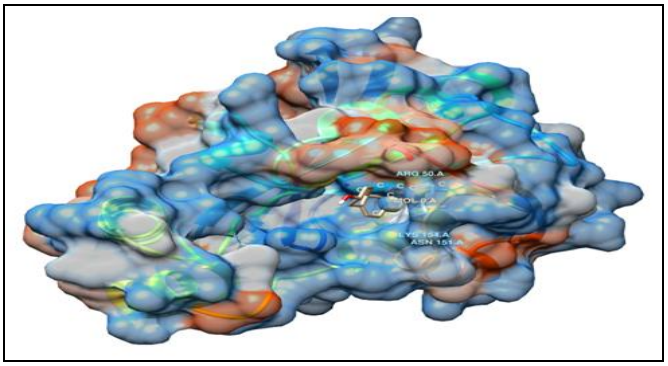

FIG. 18: DEPICTION OF β- INTEGRATED IN *TOXB* BINDING POCKET VISUALIZED UPON REPRESEN-TATION OF *TOXB* IN HYDROPHOBICITY SURFACE MODEL, INTEGRATION OF β-SITOSTEROL DEEP INTO THE BINDING POCKET IS VISUALIZED BY INCREASED TRANSPARENCY OF HYDROPHOBICITY SURFACE

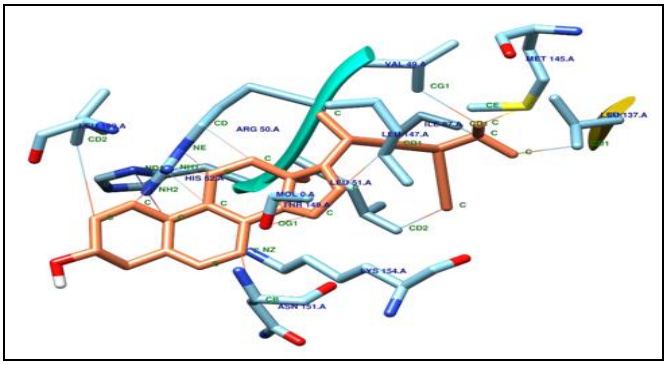

FIG. 19: MOLECULAR INTERACTION OF β-SITOSTEROL WITH AMINO ACID RESIDUES OF THE BINDING SITE WHERE THE ATOMS INVOLVED IN BOND FORMATION AND THE RESIDUE NUMBERS HAVE BEEN LABELLED IN GREEN AND BLUE RESPECTIVELY

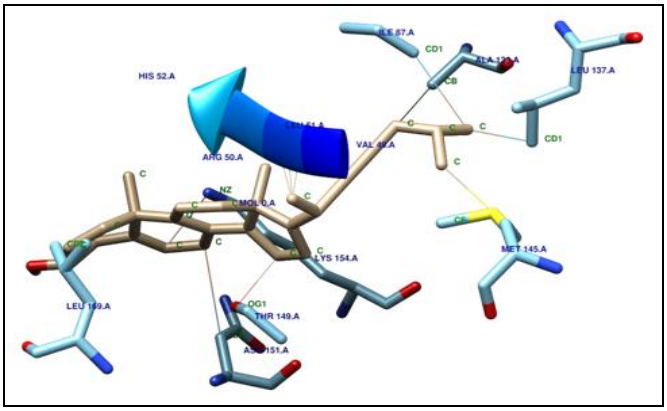

FIG. 20: MOLECULAR INTERACTION OF β-SITOSTEROL WITH AMINO ACID RESIDUES OF THE BINDING SITE DEPICTED FROM HIND SIGHT VIEW, WHERE THE ATOMS INVOLVED IN BOND FORMATION AND THE RESIDUE NUMBERS HAVE BEEN LABELLED IN GREEN AND BLUE RESPECTIVELY

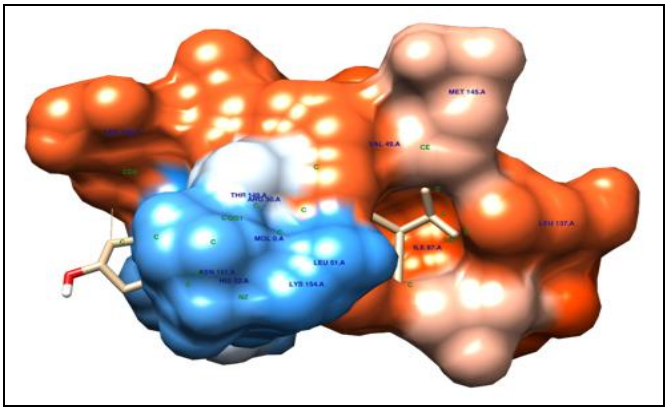

FIG. 21: EXHIBITING β-SITOSTEROL INTEGRATED IN BINDING POCKET OF *TOXB*, WHERE BINDING POCKET OF *TOXB* IS EXCLUSIVELY DEPICTED IN HYDROPHOBICITY SURFACE MODEL

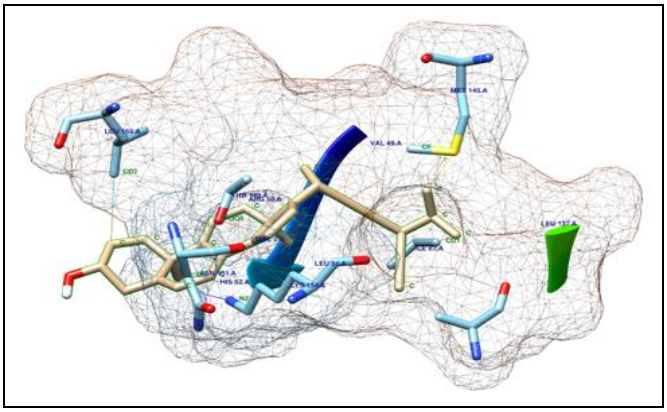

FIG. 22: EXHIBITING β-SITOSTEROL INTEGRATED IN BINDING POCKET OF *TOXB*, WHERE BINDING POCKET OF *TOXB* IS EXCLUSIVELY DEPICTED IN HYDROPHOBICITY SURFACE MESH MODEL

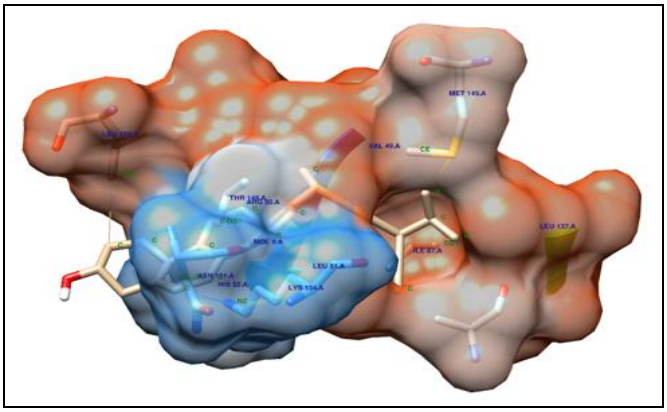

FIG. 23: EXHIBITING B-SITOSTEROL INTEGRATED IN BINDING POCKET OF *TOXB*, WHERE BINDING POCKET OF *TOXB* IS EXCLUSIVELY DEPICTED IN HYDROPHOBI-CITY SURFACE MODEL, WHERE DEEP INTEGRATION OF B-SITOSTEROL CAN BE VISUALIZED UPON INCREASING THE TRANSPARENCY OF HYDROPHOBICITY MODEL

Interaction of β-sitosterol with *DnaA:* β-sitosterol was found to bind *DnaA* at a binding site specified above along with additional amino acid residues surrounding the binding site of *DnaA*, overall of β-sitosterol was found to interact with TYR114, THR152, GLY153, LYS156, THR157, HIS158, ILE281, and ILE309 as shown from **Fig. 24 - Fig. 30**.

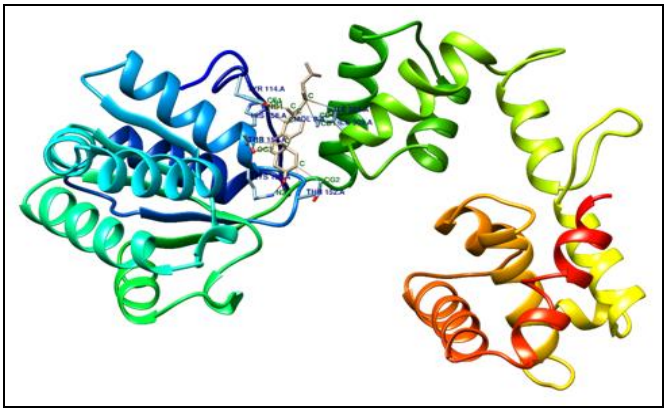

FIG. 24: MOLECULAR INTERACTION OF β-SITOSTEROL WITH *DNAA* BINDING SITE DEPICTED IN RIBBON PRESET WITH β-SITOSTEROL DEPICTED IN GOLDEN HUE

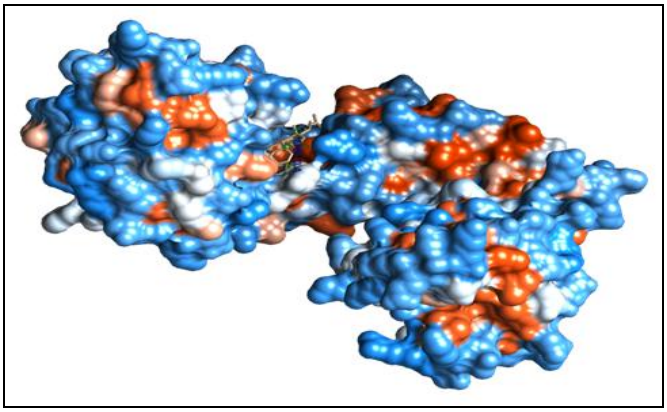

FIG. 25: DEPICTION OF B-SITOSTEROL INTEGRATED IN *DNAA* BINDING POCKET VISUALIZED UPON REPRESENTATION OF *DNAA* IN HYDROPHOBICITY SURFACE MODEL

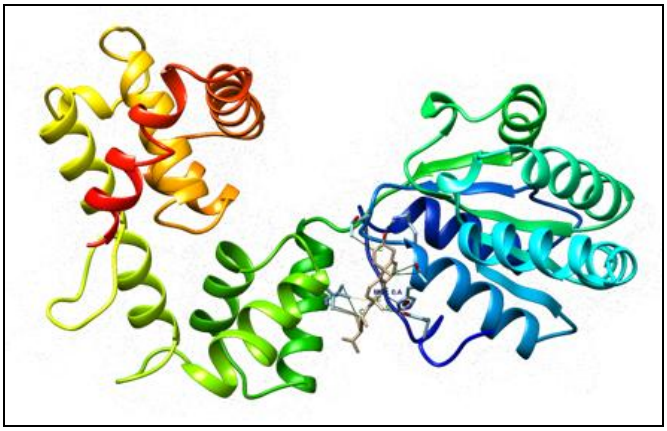

FIG. 26: DEPICTION OF β-SITOSTEROL INTEGRATED IN *DNAA* BINDING POCKET VISUALIZED UPON REPRESENTATION OF β-SITOSTEROL IN CYLINDER MODEL AND *DNAA*IN DOTTED HYDROPHOBICITY SURFACE

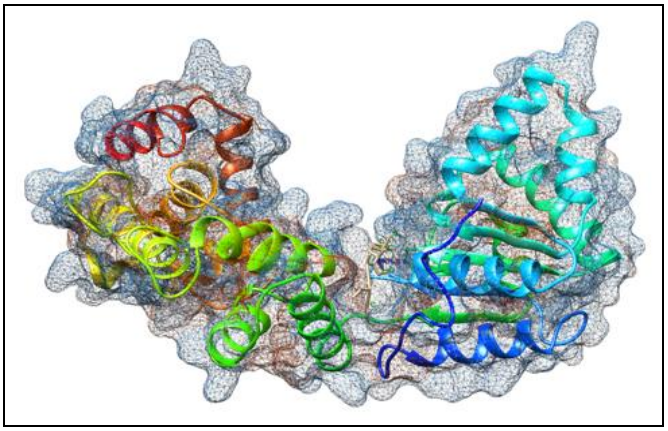

FIG. 27: DEPICTION OF β-SITOSTEROL INTEGRATED IN *DNAA* BINDING POCKET VISUALIZED UPON REPRESENTATION OF *DNAA* IN HYDROPHOBICITY SURFACE MESH MODEL, WHERE β-SITOSTEROL IS DEPICTED IN CYLINDER MODEL WITH GOLDEN HUE

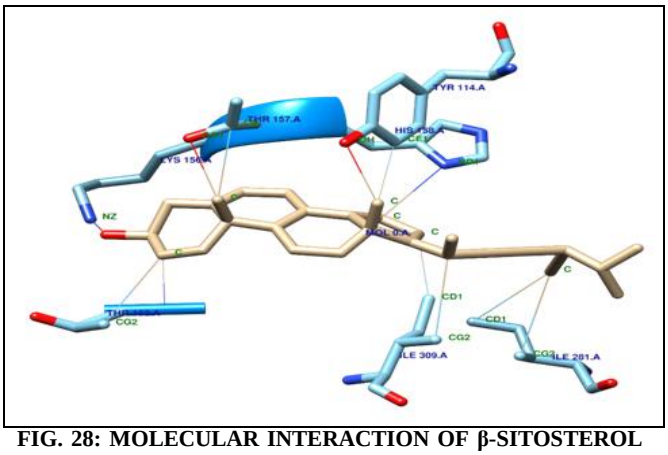

FIG. 28: MOLECULAR INTERACTION OF β-SITOSTEROL WITH AMINO ACID RESIDUES OF THE BINDING SITE OF *DNAA* WHERE THE ATOMS INVOLVED IN BOND FORMATION AND THE RESIDUE NUMBERS HAVE BEEN LABELLED IN GREEN AND BLUE RESPECTIVELY

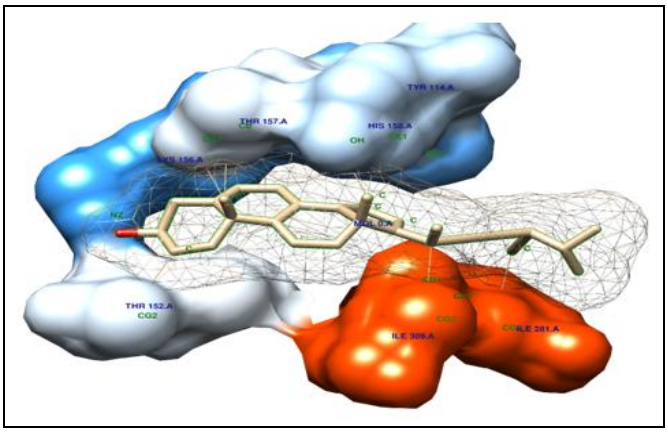

FIG. 29: EXHIBITING β-SITOSTEROL INTEGRATED IN BINDING POCKET OF *DNAA*, WHERE BINDING POCKET OF *DNAA* IS EXCLUSIVELY DEPICTED IN SOLID HYDROPHOBICITY SURFACE MODE

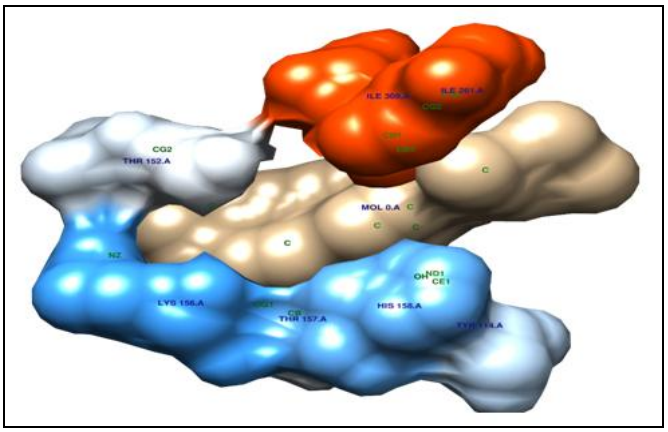

FIG. 30: EXHIBITING B-SITOSTEROL INTEGRATED IN BINDING POCKET OF *DNAA* DEPICTED IN HYDROPHOBICITY SURFACE WITH GOLDEN HUE, WHERE BINDING POCKET OF *DNAA* IS ALSO DEPICTED IN SOLID HYDROPHOBICITY SURFACE MODE

Interaction of β-sitosterol with *PhnB*: β-sitosterol was found to bind *PhnB* at a binding site specified above along with additional amino acid residues surrounding the binding site of *PhnB*, overall of β-sitosterol was found to interact with ASN8, ASN32, ILE54, GLY59, SER63, SER64, LEU67, ILE71, GLY86, LEU87, and ALA89 as shown in the **Fig. 31 - Fig. 37**.

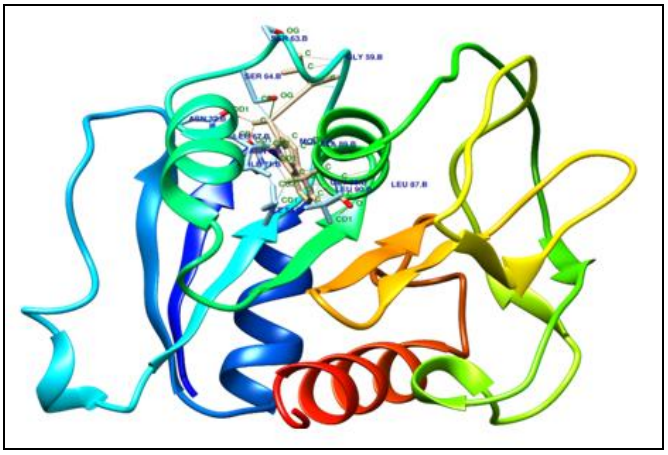

FIG. 31: MOLECULAR INTERACTION OF β-SITOSTEROL WITH *PHNB* BINDING SITE DEPICTED IN RIBBON PRESET WITH β-SITOSTEROL DEPICTED IN GOLDEN HUE

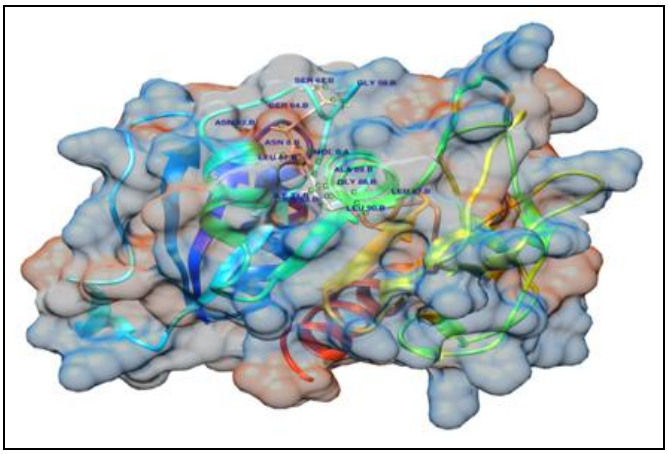

FIG. 32: DEPICTION OF β-SITOSTEROL INTEGRATED INTO *PHNB* BINDING POCKET VISUALIZED UPON THE REPRESENTATION OF *PHNB* IN HYDROPHOBICITY SURFACE MODEL, INTEGRATION OF β-SITOSTEROL DEEP INTO THE BINDING POCKET IS VISUALIZED BY INCREASED TRANSPARENCY OF HYDROPHOBICITY SURFACE

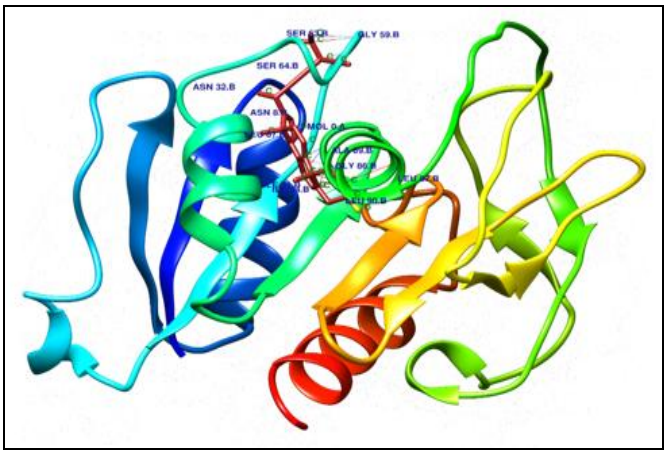

FIG. 33: DEPICTION OF β-SITOSTEROL INTEGRATED INTO *PHNB* BINDING POCKET VISUALIZED UPON THE REPRESENTATION OF β-SITOSTEROL IN-CYLINDER MODEL DEPICTED IN BRICK RED HUE AND *PHNB*IN DOTTED HYDROPHOBICITY SURFACE

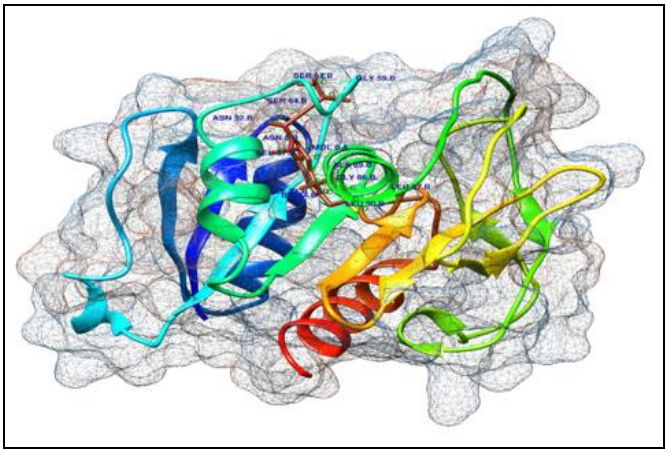

FIG. 34: DEPICTION OF β-SITOSTEROL INTEGRATED INTO *PHNB* BINDING POCKET VISUALIZED UPON THE REPRESENTATION OF *PHNB* IN HYDROPHOBICITY SURFACE MESH MODEL, WHERE β-SITOSTEROL IS DEPICTED IN-CYLINDER MODEL WITH A BRICK RED HUE

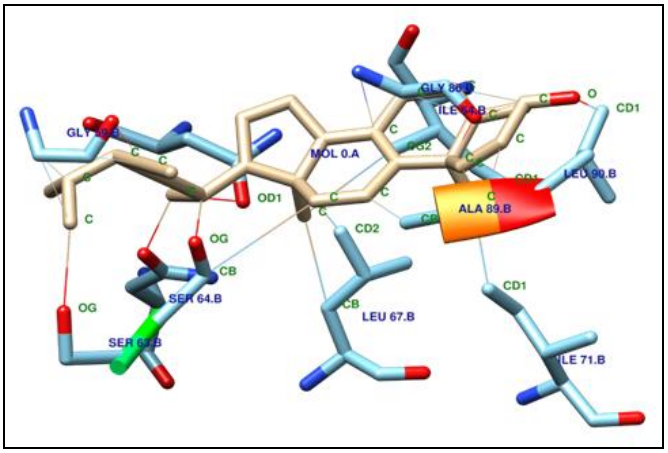

FIG. 35: MOLECULAR INTERACTION OF β-SITOSTEROL WITH AMINO ACID RESIDUES OF THE BINDING SITE OF *PHNB* WHERE THE ATOMS INVOLVED IN BOND FORMATION AND THE RESIDUE NUMBERS HAVE BEEN LABELED IN GREEN AND BLUE RESPECTIVELY

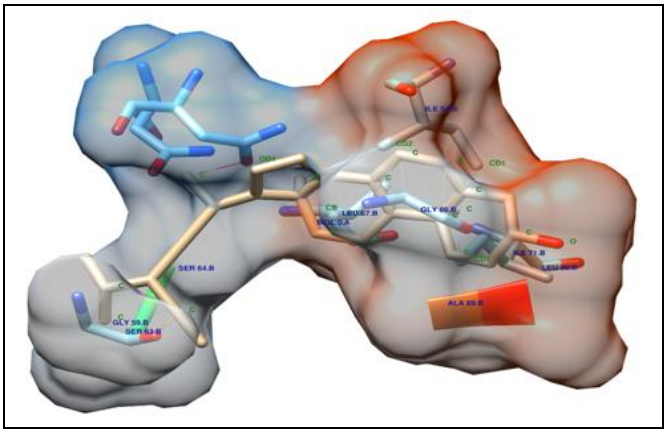

FIG. 36: EXHIBITING β-SITOSTEROL INTEGRATED INTO THE BINDING POCKET OF *DNAA*, WHERE A BINDING POCKET OF DNAA IS EXCLUSIVELY DEPICTED IN SOLID HYDROPHOBICITY SURFACE MODE

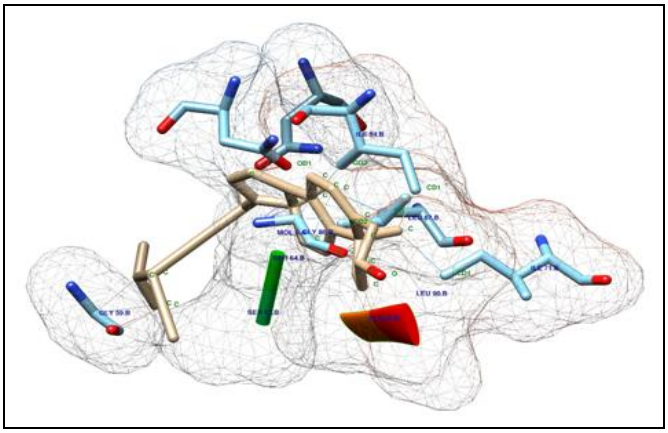

FIG. 37: EXHIBITING β-SITOSTEROL INTEGRATED INTO THE BINDING POCKET OF *PHNB*, WHERE A BINDING POCKET OF PHNB IS EXCLUSIVELY DEPICTED IN THE HYDROPHOBICITY SURFACE MESH MODEL

Interaction of β-sitosterol with *Sip*: β-sitosterol was found to bind *Sip* at a binding site specified above along with amino acid residues surrounding the binding site of *Sip*, overall of β-sitosterol was found to interact with THR119, ASN120, GLU121, TYR136, ASN189 and PHE203 as shown in the **Fig. 38 – Fig. 44**.

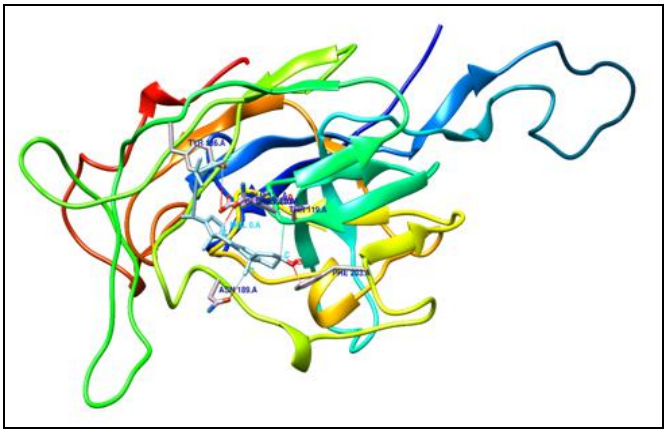

FIG. 38: MOLECULAR INTERACTION OF β-SITOSTEROL WITH SIP BINDING SITE DEPICTED IN RIBBON PRESET WITH β-SITOSTEROL DEPICTED IN A LIGHT BLUE HUE

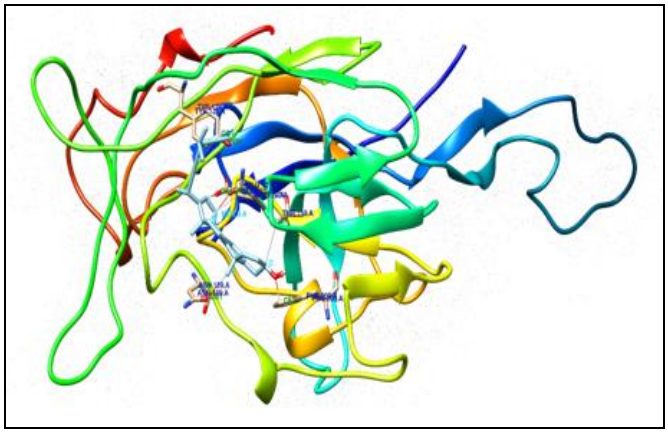

FIG. 39: DEPICTION OF β-SITOSTEROL INTEGRATED INTO *SIP* BINDING POCKET VISUALIZED UPON THE REPRESENTATION OF β-SITOSTEROL IN-CYLINDER MODEL DEPICTED IN LIGHT BLUE HUE AND *SIP* IN DOTTED HYDROPHOBICITY SURFACE

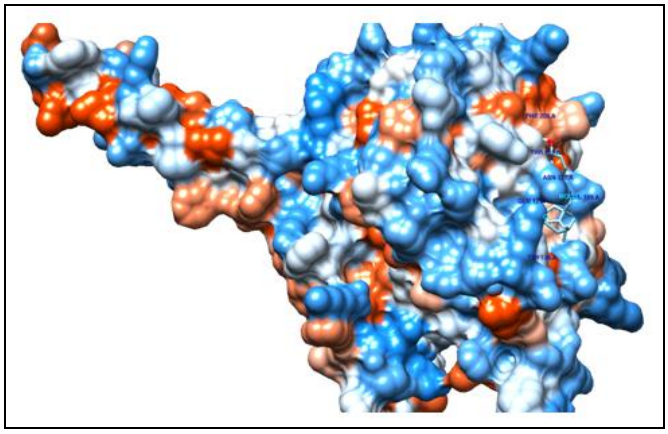

FIG. 40: DEPICTION OF β-SITOSTEROL INTEGRATED INTO *SIP* BINDING POCKET VISUALIZED UPON THE REPRESENTATION OF *SIP* IN THE HYDROPHOBICITY SURFACE MODEL

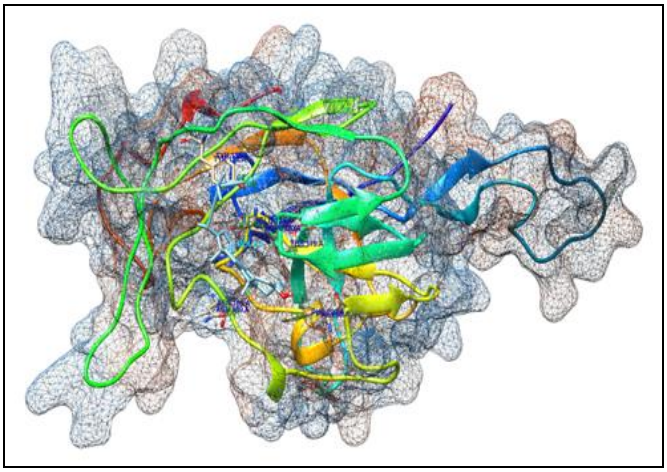

FIG. 41: DEPICTION OF β-SITOSTEROL INTEGRATED INTO *SIP* BINDING POCKET VISUALIZED UPON THE REPRESENTATION OF *SIP* IN THE HYDROPHOBICITY SURFACE MESH MODEL, WHERE β-SITOSTEROL IS DEPICTED IN-CYLINDER MODEL WITH A LIGHT BLUE HUE

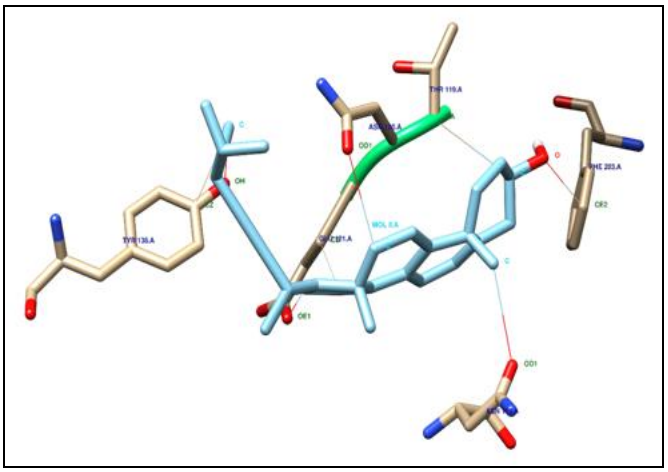

FIG. 42: MOLECULAR INTERACTION OF β-SITOSTEROL WITH AMINO ACID RESIDUES OF THE BINDING SITE OF *SIP* WHERE THE ATOMS INVOLVED IN BOND FORMATION AND THE RESIDUE NUMBERS HAVE BEEN LABELED IN GREEN AND BLUE RESPECTIVELY

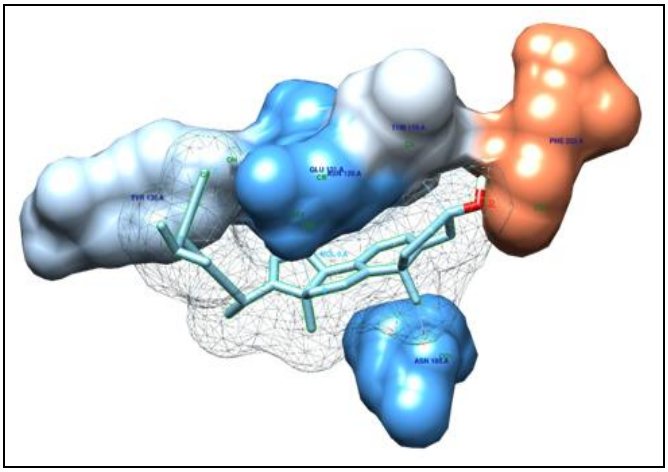

FIG. 43: EXHIBITING β-SITOSTEROL INTEGRATED INTO THE BINDING POCKET OF *SIP*, WHERE A BINDING POCKET OF SIP IS EXCLUSIVELY DEPICTED IN SOLID HYDROPHOBICITY SURFACE MODEL

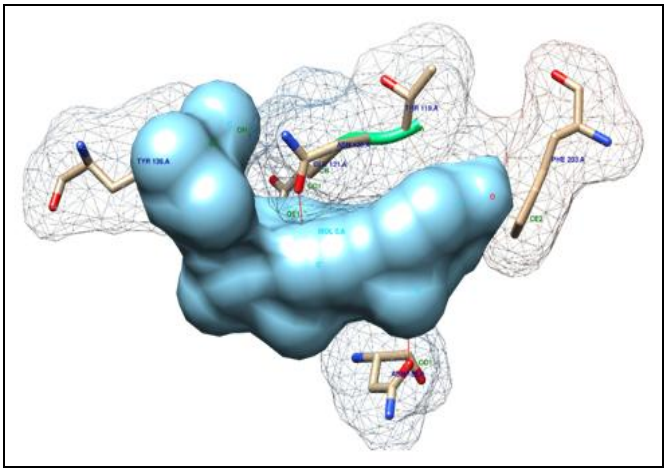

FIG. 44: DEPICTION OF β-SITOSTEROL INTEGRATED INTO *SIP* BINDING POCKET VISUALIZED UPON THE REP-RESENTATION OF β-SITOSTEROL IN HYDROPHOBICITY SOLID SURFACE MODEL AND *SIP* IN THE HYDRO-PHOBICITY SURFACE MESH MODE

CONCLUSION: Molecular interaction studies reveal that the ability of *Acarus calamus* in inhibiting biofilm formation in *H. pylori* might be due to the inhibitory effect of phytobio-active component, β-sitosterol, against quorum sensing molecules- *ToxB, DnaA, PhnB,* and *Sip*, making it a novel therapeutic alternative to treat *H. pylori* infections.

ACKNOWLEDGEMENT: Authors acknowledge the Head of the Institute, JSS Academy of Higher Education, Mysuru, for the facilities. C. S. greatly acknowledges the funding support from DST DST-SERB (YSS/2015/001135/LS (Ver-I).

CONFLICTS OF INTEREST: The authors declare no conflict of interest.

REFERENCES:

1. Shin JM, Vagin O, Munson K, Kidd M, Modlin IM and Sachs G: Molecular mechanisms in therapy of acid-related diseases. Cell Mol Life Sci 2008; 65: 264-81.
2. Abadi TB, Ierardi E and Lee J: Why do we still have *Helicobacter pylori* in our Stomachs? Malays J Med Sci 2015; 22: 70-75.
3. Megraud F, Coenen S, Versporten A, Kist M, Lopez-Brea M, Hirschl AM, Andersen LP, Goossens H and Glupczynski Y: *Helicobacter pylori* resistance to antibiotics in Europe and its relationship to antibiotic consumption. Gut 2013; 62: 34-42.
4. Arshad M, Akram M, Shahab-uddin, Afzal A, Khan U and Abdul H: *Helicobacter pylori*: an introduction 2010; 1(3): 0976-4550.
5. Farrell S, Doherty GM, Milliken I and Shield MD: Risk factors for *Helicobacter pylori* infection in children: an examination of the role played by intrafamilial bed sharing. McCallion WAP ediatr Infect Dis J 2005; 24(2): 149-52.

6. The EUROGAST Study Group: Epidemiology of, and risk factors for, *Helicobacter pylori* infection among 3194 asymptomatic subjects in 17 populations. Gut 1993; 34: 1672-76.
7. Pounder RE and Ng D: The prevalence of *Helicobacter pylori* infection in different countries. Aliment Pharmacol Ther 1995; 9(S2): 33-39.
8. Kuppusamy P, Yusoff MM, Maniam GP and Govindan N: Biosynthesis of metallic nanoparticles using plant derivatives and their new avenues in pharmacological applications-An updated report. Saudi Pharm J 2016; 24: 473-84.
9. Jain S and Mehata MS: Medicinal plant leaf extract and pure flavonoid mediated green synthesis of silver nanoparticles and their enhanced antibacterial property Sci Rep 2016; 7: 158-67.
10. Withers HL and Nordstro MK: Quorum-sensing acts at initiation of chromosomal replication in *Escherichia coli*. Proc Natl Acad Sci USA 1998; 95: 15694-99.
11. Wen Y, Marcus EA, Matrubutham U, Gleeson MA, Scott DR and Sachs G: Acid-adaptive genes of *Helicobacter pylori*. Infection and Immunity 2003: 71: 5921-39.
12. Zhang Y: I-TASSER server for protein 3D structure prediction, BMC Bioinformatics 2008; 9: 40-47.
13. Roy A, Kucukural A and Zhang Y: I-TASSER: a unified platform for automated protein structure and function prediction, Nature Protocols 2010; 5: 725-38.
14. Yang J, Yan R, Roy A, Xu D, Poisson J and Zhang Y: The I-TASSER Suite: protein structure and function prediction. Nature Methods 2015; 12: 7-8.
15. Open Babel Python [http://openbabel.sourceforge.net/wiki/Python].
16. Cosconati S: Virtual Screening with AutoDock: Theory and Practice. Expert Opin Drug Discov 2010; 5: 597-607.
17. Pettersen EF, Goddard TD, Huang CC, Couch GS, Greenblatt DM, Meng EC and Ferrin TE: UCSF Chimera-A visualization system for exploratory research and analysis. J of Computational Chemistry 2004; 25: 1605-12.

How to cite this article:
Prasad A, Shruthi G, Sushma P, Jain AS, Chandan D, Prasad MNN, Kollur SP, Chandrashekar S and Shivamallu C: *Helicobacter pylori* infection: a bioinformatic approach. Int J Pharm Sci & Res 2020; 11(11): 5469-83. doi: 10.13040/IJPSR.0975-8232.11(11).5469-83.